J Plant Growth Regul (2007) 26:229–244
DOI 10.1007/s00344-007-9011-x

Cytokinin Regulation of Gene Expression in the *AHP* Gene Family in *Arabidopsis thaliana*

Jana Hradilová · Jiří Malbeck · Břetislav Brzobohatý

Received: 28 August 2006 / Accepted: 18 January 2007 / Published online: 27 August 2007

Abstract In higher plants histidine-aspartate phosphorelays are involved in hormone and stress signaling via a two-component system of signal transduction. In this system a histidine-containing phosphotransmitter (HPt) mediates signal transmission from a sensory histidine kinase to a response regulator, providing integration and/or branching of several different signaling pathways. Five genes encoding HPts, *AHP1-5*, have been identified in *Arabidopsis*. Histidine-aspartate phosphorelays involving HPts have been at least partly implicated in cytokinin signaling. We analyzed the regulation by cytokinins of *AHP* gene expression. We compared the effects on steady–state levels of *AHP* transcripts of a short-term treatment with an aromatic cytokinin and increase in endogenous isoprenoid cytokinin levels using an activable *ipt* system in 8-day-old *Arabidopsis* seedlings. Following *ipt* activation, a rapid and highly preferential increase in *trans*-zeatin-type cytokinins was observed, whereas other isoprenoid-type cytokinins showed no or only marginal increases. The levels of cytokinin metabolites under long-term *ipt* activation suggest that the seedlings may have difficulties in efficiently downregulating active forms of the hormone. Using real-time RT-PCR, transient increases in steady-state levels of *AHP1-4* transcripts in response to both the short-term N^6-benzyladenine treatment and the increase in endogenous *trans*-zeatin-type cytokinin levels were observed. In contrast, both the full and the alternatively spliced *AHP5* transcripts remained unaltered. On the other hand, increases in steady-state levels of *AHP1-4* transcripts observed in seedlings cultivated continuously in the presence of exogenous N^6-benzyladenine were not paralleled in seedlings with constitutively increased endogenous *trans*-zeatin-type cytokinins, providing further indirect evidence for distinct functions of aromatic and isoprenoid cytokinins.

Keywords Gene expression · *AHP* gene family · Cytokinin signal transduction · Cytokinin metabolism · Isopentenyl transferase

J. Hradilová · B. Brzobohatý (✉)
Institute of Biophysics, Academy of Sciences of the Czech Republic, Královopolská 135, CZ-61265 Brno, Czech Republic
e-mail: brzoboha@ibp.cz

J. Hradilová · B. Brzobohatý
Department of Molecular Biology and Radiobiology, Faculty of Agronomy, Mendel University of Agriculture and Forestry, Zemědělská 1, CZ-61300 Brno, Czech Republic

J. Malbeck
Institute of Experimental Botany, Academy of Sciences of the Czech Republic, Rozvojová 135, CZ-16502 Prague, Czech Republic

Introduction

Cytokinins (CKs) are plant hormones implicated, along with other plant hormones, in the regulation of a plethora of responses in plants, including meristem activity, *de novo* bud formation, release from apical dominance, leaf expansion, reproductive development, and senescence (Binns 1994; Brzobohatý and others 1994; Mok and Mok 2001).

Naturally occurring CKs are adenine derivatives substituted at the N^6 position with an isoprenoid or aromatic side chain. Isoprenoid CKs are the predominant natural form of CKs, whereas aromatic CKs, including N^6-benzyladenine (BA), represent a minor component of the CK pool (Strnad 1997; Sáenz and others 2003). Genes, for

example, *tzs* and *ipt*, encoding enzymes for the biosynthesis of isoprenoid CKs were first cloned from *Agrobacterium tumefaciens* (Akiyoshi and others 1984; Barry and others 1984), although no biosynthetic enzyme was found for aromatic CKs. The enzyme isopentenyl transferase (IPT) converted AMP and dimethyallyl-pyrophosphate (DMAPP) to the free CK N^6-(Δ^2-isopentenyl)adenosine-5′-monophosphate (iPMP). However, recent work (Åstot and others 2000; Sakakibara and others 2005) has provided strong evidence for an iPMP-independent CK biosynthesis pathway leading directly to zeatin (Z)-type CKs that apparently predominate in plants expressing the *ipt* gene. Plant IPTs were best characterized in *Arabidopsis* whose genome encodes nine family members (*AtIPT1* to *AtIPT9*; Kakimoto 2001; Takei and others 2001). In contrast to bacterial *ipt*, overexpression of *AtIPT*s in *Arabidopsis* leads to the accumulation of isopentenyl (iP)-type CKs (Sun and others 2003; Sakakibara and others 2005). Postbiosynthesis steps of the CK metabolism pathway are also being elucidated by cloning and characterization of several genes encoding enzymes involved in CK metabolism, like cytokinin hydroxylases (CYP735A1 and CYP735A2) that catalyze hydroxylation of iP to *t*-Z at the nucleotide level (Takei and others 2004); CK oxidase/dehydrogenase (Houba-Hérin and others 1999; Morris and others 1999; Werner and others 2003) that cleaves the N^6 side chain from CKs; and enzymes that catalyze the conjugation of sugar moieties to CKs (Martin and others 1999a, 1999b, 2001; Hou and others 2004), as well as release of free CKs from their *O*-glucosides (Brzobohatý and others 1993; Kiran and others 2006).

A model for CK perception has emerged that is similar to the prokaryotic two-component response pathways (Haberer and Kieber 2001; Hutchinson and Kieber 2002; Lohrmann and Harter 2002; Grefen and Harter 2004). Genetic screens, genetic studies in His kinase-deficient yeast, and *in vitro* CK binding assays have demonstrated that *AHK2*, *AHK3*, and *AHK4/CRE1/WOL* act as CK receptors (Inoue and others 2001; Suzuki and others 2001a; Ueguchi and others 2001; Yamada and others 2001), and the CKI1 histidine kinase might apparently constitutively activate CK signaling (Kakimoto 1996). These receptors may act through other two-component elements, including *Arabidopsis* homologs of histidine-containing phosphotransmitters (AHPs) that are expected to transduce the signal by transferring a phosphoryl group from the transmitting domain of an activated histidine kinase to the receiver domain of type-B response regulators (ARRs), which are involved in the upregulation of type-A ARRs (Hwang and Sheen 2001; Sakai and others 2001). The completion of the *Arabidopsis* genome uncovered a highly homologous family of five *AHP* genes (Miyata and others 1998; Suzuki and others 1998, 2000) that were capable of undergoing phosphorylation at an essential histidine residue and transferring a phosphoryl group to the receiver domain of ARRs (Suzuki and others 1998, 2001b; Imamura and others 1999, 2001). Genome searches have revealed a sixth gene, *AHP6*, in which the essential histidine residue in the phosphorylation motif is replaced by an asparagine (Suzuki and others 2000) and is therefore occasionally called a pseudo-HPt. Analyses of the expression pattern of *AHP* genes revealed that their transcripts are present in all *Arabidopsis* organs, although at different levels (Miyata and others 1998; Tanaka and others 2004; Hradilová and Brzobohatý 2007). Recent analysis in our group has uncovered the presence of two *AHP5* transcripts. In addition to the predominant transcript corresponding to the fully spliced *AHP5* mRNA, an alternatively spliced variant retains unspliced the second intron of the *AHP5* gene. Expression of *AHP1*, *AHP2*, and *AHP4* is highly organ-specific, whereas that of *AHP3* and *AHP5* appears more ubiquitous. Interestingly, the fraction of alternatively spliced *AHP5* transcripts apparently differs in the individual organs of *Arabidopsis* (Hradilová and Brzobohatý 2007).

Several lines of independent evidence suggest a role for AHPs in CK signaling: (i) in yeast two-hybrid assays AHP1-3 interact physically with the histidine kinases AHK4/CRE1/WOL or CKI1 as well as with several type-B ARRs; (ii) *in vitro* biochemical assays prove the transfer of a phosphoryl group during these interactions (Imamura and others 1999; Suzuki and others 2001a); (iii) *in vivo* localization of the GFP/AHP1-4 fusion proteins shows the transient transfer of these HPts from the cytoplasm to the nucleus in a CK-dependent manner (Hwang and Sheen 2001; Imamura and others 2001); (iv) *AHP2* ectopic expression in transgenic plants leads to CK hypersensitivity (Suzuki and others 2002); (v) silencing of a gene encoding an HPt protein turns off a CK signaling circuit in *Catharanthus roseus* suspension cells (Papon and others 2004). Very recently, AHP6 was shown to counteract CK signaling in the regulation of cell fate during root vascular development (Mähönen and others 2006).

ARR4 and *ARR5* genes were the first primary CK response genes identified (Brandstatter and Kieber 1998), and later analyses, including genome-wide expression profiling, show that the same is true for several other members of the type-A *ARRs* (D'Agostino and others 2000; Hoth and others 2003; Rashotte and others 2003; Brenner and others 2005). Expression of the CK receptor *AHK4/CRE*1 was found to be upregulated by CKs [though with slower kinetics (Hoth and others 2003; Rashotte and others 2003)] and downregulated in CK-deficient *Arabidopsis* seedlings (Brenner and others 2005). Similarly, an increase in *CKI1* expression was apparent after only 12 h and

reached a maximum after 24 h of CK treatment (Hejátko and others, unpublished results). Interestingly, Mähönen and others (2006) observed downregulation of *AHP6* transcripts after a 6-h treatment with CKs, and expansion of *AHP6* expression pattern in CK receptor mutants. Except for *AHP5* (Hoth and others 2003), *AHP* genes were scored as CK-insensitive (Rashotte and others 2003; Hoth and others 2003; Brenner and others 2005). However, the published expression data point to CK upregulation for other *AHP* genes, although below the cutoff limits used in the genome-wide analyses. Hence, we reexamined steady-state levels of the *AHP* transcripts in response to short- and long-term CK action by real-time RT-PCR. We compared the effects of exogenous administration of an aromatic CK and increased levels of endogenous CKs achieved using an inducible *ipt* expression system (Craft and others 2005). We analyzed the dynamics of the CK pool upon *ipt* induction as a basis for the correct interpretation of *AHP* expression data with respect to the kinetics and the CK types involved. We gained novel insights into CK metabolism in *Arabidopsis* seedlings.

Materials and Methods

Plant Material and Growth Conditions

Transgenic plants *CaMV35S > GR > ipt* (pOp^{BK}-ipt line 11; Craft and others 2005) and the corresponding wild-type *Arabidopsis thaliana* (ecotype Columbia 0) were used in this work. *Arabidopsis* seeds were grown on solid Murashige-Skoog (MS) medium supplemented with 1% sucrose, adjusted to pH 5.7 prior to autoclaving, and solidified with 1% agar (Duchefa, The Netherlands) in plastic Petri plates (9-cm diameter). To synchronize germination, plates with seeds were kept in darkness at 4°C for 48 h and subsequently transferred into a growth chamber (AR-36L Percival) and incubated at 21°C day/19°C night and at a 8 h day/16 h night photoperiod with a photosynthetic photon flux density of approximately 100 μmol m^{-2} s^{-1} provided by cool white fluorescent lamps.

Dexamethasone and Benzyladenine Treatments

Dexamethasone (DEX; Sigma-Aldrich, St. Louis, MO, USA) and benzyladenine (BA; Duchefa, The Netherlands) were dissolved at 20 mM and 50 mM in ethanol and 1 M NaOH, respectively, and kept at −20°C and 4°C, respectively. For DEX treatments, we used 20 μM DEX diluted from the 20 mM stock in 96% ethanol (Lachema, Czech Republic). An equal volume of ethanol was added as a solvent control to a final concentration of 0.096% (v/v) ethanol in MS media. For BA treatments, MS medium was supplemented with 2.5, 5.0, 7.5, and 10.0 μM BA from 50 mM stock in 1 M NaOH. An equal volume (with respect to 10.0 μM BA) of 1 M NaOH was added as a solvent control to a final concentration of 0.2 mM NaOH in MS media. pH was readjusted to 5.7 prior to autoclaving when necessary. For long-term treatments, seedlings were germinated and grown on MS media containing the desired concentration of DEX or BA for 8 days under the cultivation conditions given above. For short-term treatments, seedlings were germinated and grown on MS plates for 7 days and transferred to the appropriate medium during the 8th day according to a schedule that ensured the completion of every treatment by the end of the 8th day. For induction in liquid medium, up to 100 seedlings were transferred from MS plates to conical flasks (250 ml) containing 100 ml MS medium. Cultivation conditions were the same as above. At the end of the 8th day, seedlings were harvested, blotted dry (for treatments in liquid MS), and frozen in liquid nitrogen before RNA and CK extractions.

RNA Isolation

Total RNA was extracted from the collected material using Trizol reagent (Invitrogen, Germany) following the manufacturer's recommended procedure for 100 mg fresh tissue. The residual DNA was removed by treating with RNase-free DNaseI (Roche, Switzerland). Subsequently, DNaseI was inactivated at 70°C/10 min and the treated RNA was purified using ethanol precipitation with 3 M sodium acetate, pH 5.2, and washing with 75% ethanol. Isolated RNA was dissolved in an appropriate volume of RNase-free water and stored at −80°C.

Real-time RT-PCR Experiments

A two-step procedure was used for real-time RT-PCR. In the reverse transcription step, the oligo-dT primer RTP3 (CGT TCG ACG GTA CCT ACG TTT TTT TTT TTT TTT TT) was employed to prime the reverse transcription reaction using 5 μg total RNA and SuperScript II RNase H^- Reverse Transcriptase (Invitrogen) according the supplier's recommended procedure (denaturation at 70°C/10 min, cDNA synthesis at 42°C/52 min, enzyme inactivation at 70°C/15 min). The resulting cDNA served as a template in the PCR step. To quantify the individual *AHP* and *ipt* mRNAs in *Arabidopsis* seedlings, a SYBR Green I real-time RT-PCR assay was employed. PCR amplifications were performed in a 25-μl reaction volume containing 0.2× SYBR Green I nucleic acid gel stain (Molecular Probes, USA), 0.5 μM each of upper and lower primers, 1

mM each dNTP, 5 µl cDNA, 1 U Taq DNA polymerase 1.1, and the provided buffer at the recommended concentration (Top-Bio, Czech Republic) using the Rotorgene 3000 (Corbett Research, Australia). Gene-specific primer pairs are listed in Table 1. Actin cDNA fragments amplified with ACTfwd and ACTrev (corresponding to *ACTIN2* and *ACTIN8* genes, An and others 1996; Szyroki and others 2001) were used to normalize the steady-state mRNA levels. The general PCR conditions were as follows: denaturation at 94°C for 30 s; annealing at 55°C for 30 s; extension at 72°C for 30 s; fluorescence reading at 82°C for 15 s; 35 cycles. The general procedure was optimized for each set of primers to prevent nonspecific PCR products and primer-dimer formation; the resulting modifications of the general conditions are listed in Table 1. A melting curve analysis was performed immediately after PCR by monitoring the fluorescence as the temperature was increased slowly from 50°C to 90°C. An aliquot of the PCR product was run on a 2% agarose gel to confirm that each primer pair amplified product(s) of the expected molecular mass. The identity of the PCR products was further verified by DNA sequencing. The threshold cycle was defined as the cycle at which a statistically significant increase in the fluorescence value above the threshold value was first detected. The individual gel-purified PCR fragments were used to generate calibration curves. To enable statistical analysis, two fully independent real-time RT-PCR experiments (starting with seedling cultivation) were performed and each real-time PCR sample was run in triplicate.

Statistical Analysis

The mean of the three replicates and the standard deviations were calculated for copy numbers of the individual *AHP*, *ipt*, and *ACTIN* (*ACT*) transcripts. The abundance of the *AHP* and *ipt* transcripts is presented as an *AHPn/ACT* and *ipt/ACT* copy number ratio, respectively, and a treated/nontreated ratio. The standard deviation of the ratio was calculated using the equation

$$SD = \sqrt{cv_1^2 + cv_2^2}\,, \quad \text{where} \quad cv = \frac{SD}{\overline{X}}$$

[see User Bulletin No. 2, ABI Prism 7700 Sequence Detection System (1997), Applied Biosystems, Foster City, CA]. The resulting values from the triplicates for the individual pairs of the independent real-time RT-PCR experiments (each representing one experimental treatment) were not found to be significantly different using Student's *t* test ($p = 0.05$). Thus, subsequently they were used to calculate the mean and the standard deviation that represent the individual treatment as shown in Figures 1 and 2. Student's *t* test ($p = 0.05$) was also used to assess the

Table 1 Oligonucleotides used in Real-Time RT-PCR Analysis

Gene/transcript	Primer	Sequence	Modification
AHP1	AHP1rtu	5′TAGGAGCACAGAGAGTTAAGA3′	30 cycles
At3g21510	AHP1rtl	5′GCACAAAGAAAGAAGTTCAC3′	
AHP2	AHP2rtu	5′AAAAATCCTCTCCCAATCTCC3′	30 cycles
At3g29350	AHP2rtl	5′CTTTGTCTTTAACGCCTTGTA3′	
AHP3	AHP3rtu	5′AGCTGCAAGATGAATGTAGTC3′	30 cycles
At5g39340	AHP3rtl	5′CACTTGAGGGATTCTACCAC3′	
AHP4	AHP4rtu	5′TGTTGAAGAAGTTTCCGCATTA3′	
At3g16360	AHP4rtl	5′AAGCATCCTTCCGCATTT3′	
AHP5	AHP5rtu	5′CTCTCTATTCTTCGACGACTG3′	Annealing at 55°C
At1g03430	AHP5rtl	5′GTTCTGAACATCGCAACAT3′	
AHP5i	AHP5irtu	5′CTTTGCTTACTTTAGGCTT3′	Fluorescence reading at 78°C
	AHP5irtl	5′TCCACCTGTAAACACC3′	
ACT2, ACT8	ACTfwd	5′GGTGATGGTGTGTCT3′	Annealing 54°C, 30 cycles
At3g18780, At1g49240	ACTrev	5′ACTGAGCACAATGTTAC3′	Fluorescence reading at 85°C
ipt	*IPTrtu*	5′ATCCTCCCTCAAGAATAAGC3′	Annealing at 60°C
	IPTrtl	5′CTGAAAGGAACGACGC3′	Fluorescence reading at 83°C

Modifications of the general real-time RT-PCR protocol employed for the particular primer pairs to overcome nonspecific PCR products and primer dimer formation are shown.

[a] *AHP5i* corresponds to the alternatively spliced *AHP5* transcript.

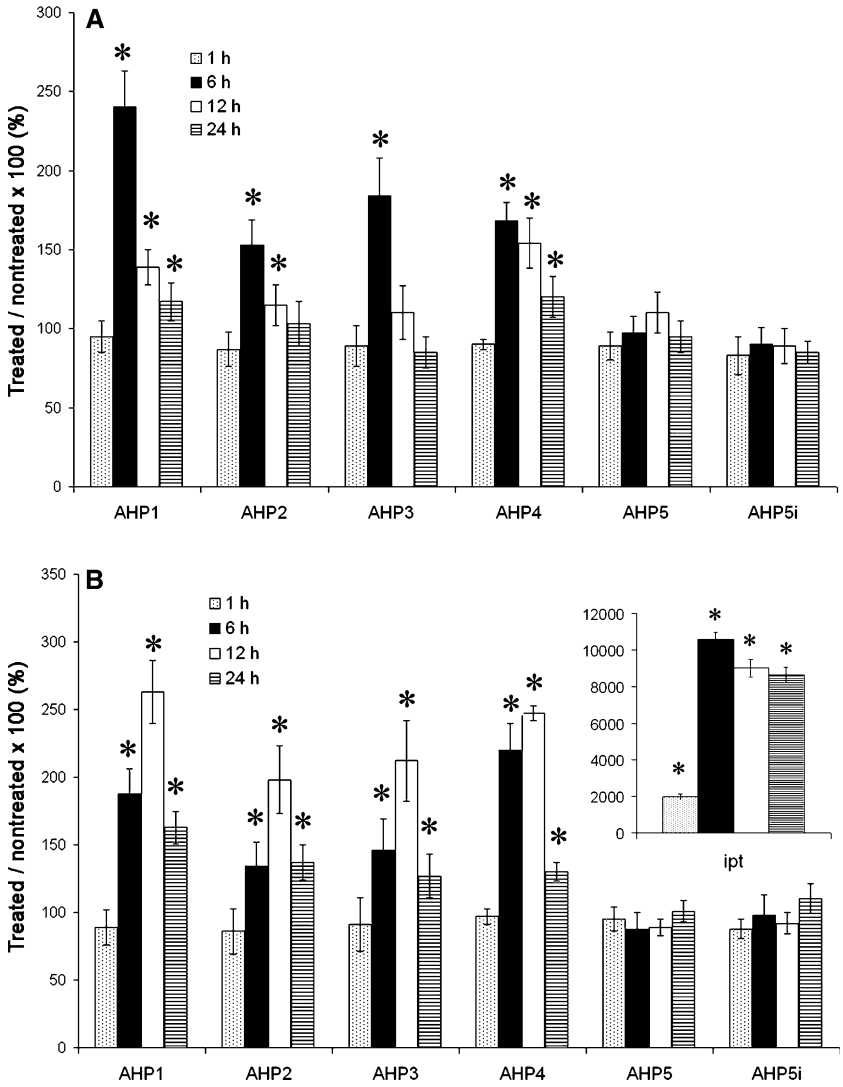

Fig. 1 Induction of *AHP* transcripts in response to a short-term CK action. Seedlings [wild-type Col 0 (**A**); pOp^{BK}-ipt line 11 (**B**)] were cultivated on MS medium and subsequently transferred into MS medium supplemented with 10 μM BA (**A**) and 20 μM DEX (**B**) for the period indicated, ensuring that the total cultivation period was 8 days. *AHP* and *ipt* transcript levels were determined by real-time RT-PCR and normalized to *ACTIN* transcripts. Levels found in treated seedlings are expressed relative to the appropriate nontreated controls. Inset in **B** shows *ipt* transcript levels in the course of DEX treatment. * marks values significantly different from nontreated seedlings at $P < 0.05$. *AHP5i* represents the alternatively spliced *AHP5* transcript

statistical significance of the differences between individual treatments.

DNA Sequencing

To confirm the identities of the RT-PCR products corresponding to the individual *AHP* mRNAs, the RT-PCR products were separated on a 2% agarose gel, DNA isolated (Qiaquick Gel Extraction Kit, Qiagen, Germany), and sequenced using the upper primers (except AHP5rtl primer) and cycle sequencing kit Big Dye Terminator (Applied Biosystems, USA) on an ABI Prism 310 Genetic Analyzer.

Sequence Analysis

Sequence analyses were performed using Biology Workbench (http://www.workbench.sdsc.edu/). The programs BLASTN, SIXFRAME, and CLUSTALW were used to analyze the nucleotide sequences. Protein sequence analysis was performed using programs CLUSTALW, PI, RPSBLAST, and AASTATS.

Extraction and Purification of CKs

The detailed procedure for extraction, purification, and quantitative analysis of CKs has been described in Lexa and others (2003). CKs were extracted overnight at –20°C with Bieleski solvent (methanol:chloroform:water:acetic acid, 12:5:2:1; Bieleski 1964) from plant tissue ground under liquid nitrogen. Deuterium-labeled CKs ($[^2H_5]$Z, $[^2H_5]$ZR, $[^2H_5]$Z-7G, $[^2H_5]$Z-9G, $[^2H_5]$Z-OG, $[^2H_5]$ZR-OG, $[^2H_3]$DZ, $[^2H_3]$DZR, $[^2H_6]$iP, $[^2H_6]$iPR, $[^2H_6]$iP-7G, $[^2H_6]$iP-9G, $[^2H_5]$ZMP, $[^2H_3]$DZMP, $[^2H_6]$iPMP; Apex, UK) were added as internal standards for MS quantification. After centrifugation, the extracts were passed through

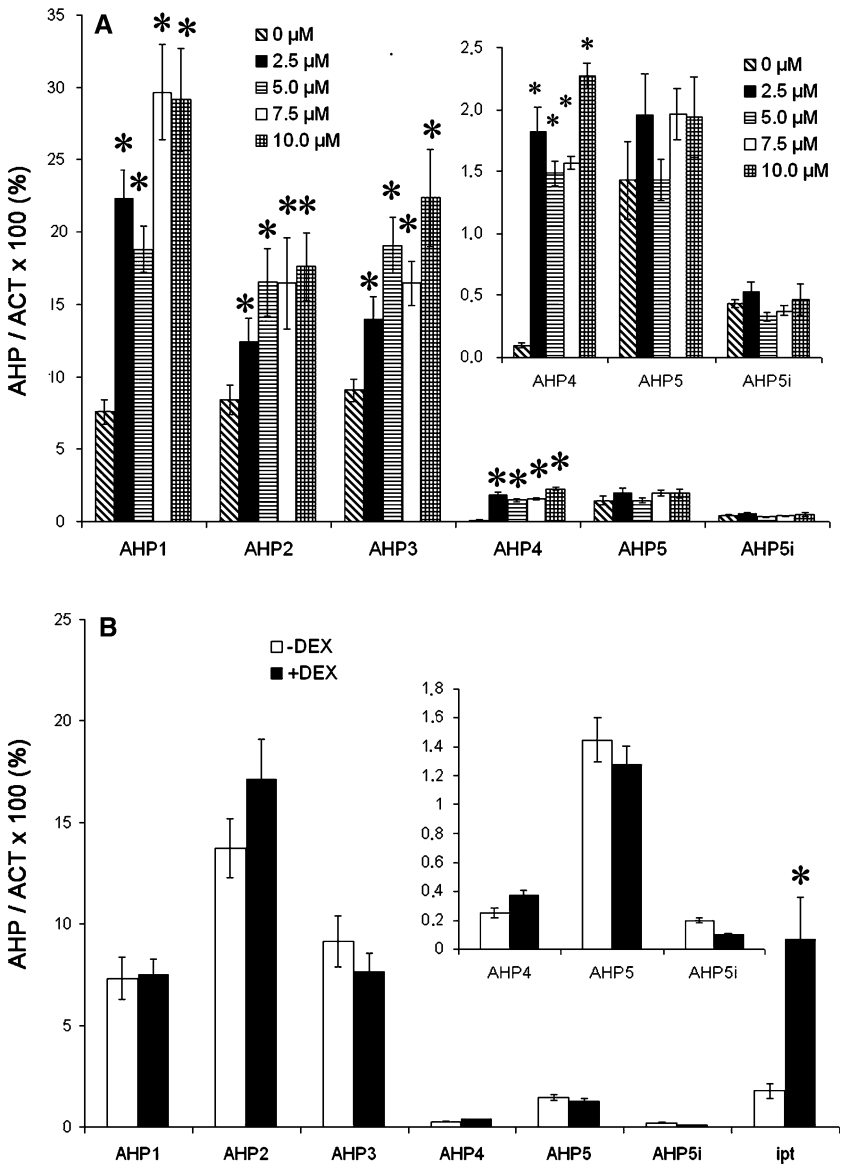

Fig. 2 Modulation of *AHP* transcripts in response to long-term CK action. Seedlings [wild-type Col 0 (A); pOp^{BK}-ipt line 11 (B)] were cultivated on MS medium supplemented with BA (**A**) at the indicated concentrations and 20 µM DEX (**B**) for 8 days. *AHP* and *ipt* transcript levels were determined by real-time RT-PCR and normalized to *ACTIN* transcripts. * marks values significantly different from nontreated seedlings at $P < 0.05$. *AHP5i* represents the alternatively spliced *AHP5* transcript

Sep-Pak C18 cartridges (Waters Corp., Milford, MA, USA) to remove pigments and lipids and evaporated to water phase. After acidifying with 5 ml of 1 M HCOOH, hormones were trapped on an Oasis MCX mixed-mode, cation-exchange, reverse-phase column (150 mg, Waters) (Dobrev and Kamínek 2002). After a wash with 1 M HCOOH, IAA and ABA were eluted with MeOH and evaporated to dryness. Furthermore, CK phosphates (CK nucleotides) were eluted with 0.34 M NH_4OH in water and CK bases, ribosides, and glucosides were eluted with 0.34 M NH_4OH in 60% (v/v) MeOH. The latter eluate was evaporated to dryness. NH_4OH was evaporated from the eluted fraction with CK nucleotides. CK nucleotides were analyzed as their corresponding ribosides after hydrolysis with alkaline phosphatase (30 min at 37°C) in 0.1 M Tris (pH 9.6) After neutralization, the solution was passed through a C18 Sep-Pak cartridge. CKs were eluted with 80% (v/v) methanol and evaporated to dryness.

Quantitative Analysis of CKs

Purified CK samples were analyzed by a LC-MS/MS system consisting of a HTS PAL autosampler (CTC Analytics, Switzerland), Rheos 2000 quaternary pump (FLUX, Switzerland) with a Csi 6200 Series HPLC Oven (Cambridge Scientific Instruments, England), and LCQ Ion Trap mass spectrometer (Finnigan, USA) equipped with an electrospray. A 10-µl sample was injected onto a C18 column (AQUA, 2 mm × 250 mm × 5 µm, Phenomenex, USA) and eluted with 0.0005% acetic acid (A) and acetonitrile (B). The gradient profile was as follows: 5 min 10% B, then

to 17% in 10 min, then to 46% in 10 min at a flow rate of 0.2 ml/min. Column temperature was kept at 30°C. The effluent was introduced in a mass spectrometer being operated in the positive-ion, full-scan MS/MS mode. Quantification was performed using a multilevel calibration graph with deuterated CKs as internal standards.

Results

Effects of Exogenous Aromatic CK Treatment on the Expression of *AHP* Genes

We examined the effects of short- and long-term CK treatment on the expression of the individual members of the *AHP* gene family by real-time RT-PCR (Figures 1A, 2A). In the short-term treatment, steady-state levels of *AHP* transcripts were assayed at 1, 6, 12, and 24 h of incubation of wild-type *Arabidopsis* seedlings in liquid MS medium supplemented with 10 μM BA. Prior to induction, *AHP1*, *AHP2*, *AHP3*, *AHP4*, *AHP5*, and *AHP5i* transcripts were found at 7.6%, 8.4%, 9.1%, 0.1%, 1.5%, and 0.4% of the *ACTIN* transcript level, respectively. No increase in steady-state transcript levels was observed within the first hour of treatment. Within the following 5 h, steady-state levels of *AHP1-4* transcripts reached a maximum and then dropped to levels comparable to untreated controls during the following 18 h. The strongest upregulation and the steepest decline were observed in *AHP1*, whereas the *AHP4* transcript level declined only slowly and remained significantly above its noninduced level even after 24 h of BA treatment. Steady-state levels of both fully and alternatively spliced *AHP5* transcripts were not changed significantly during the treatment. In the long-term treatment, the seedlings were germinated and grown on MS medium supplemented with BA at the indicated concentrations for 8 days and then steady-state levels of *AHP* transcripts were assayed. Transcript levels of *AHP1-4* genes were elevated in a dose-dependent manner. The lowest BA dose (2.5 μM) was sufficient to reach transcript levels close to saturation for *AHP4*, whereas *AHP2* and *AHP3* required 5 μM BA and *AHP1* required 7.5 μM BA. In absolute terms, the highest increase was observed for the *AHP1* transcript, reaching 30% of the *ACTIN* transcript level. However, the largest increase in transcript accumulation—25-fold—was observed for *AHP4*. Thus, *AHP4* is the most BA-responsive gene of the *AHP* gene family with respect to both the lowest dose sufficient to achieve its induction and the fold induction observed. Steady-state levels of both fully and alternatively spliced *AHP5* transcripts remained unaltered in the seedlings grown on medium supplemented with BA.

Control of *ipt* Gene Expression by the Binary pOp/LhGR System in *Arabidopsis*

We employed the binary pOp-ipt/LhGR system of dexamethasone (DEX)-inducible *ipt* expression to analyze the effects of increases in endogenous CK levels on gene expression in the *AHP* gene family. To establish *ipt* induction parameters in the pOp-ipt/LhGR system following DEX treatment, pOp^{BK}-ipt line 11 (Craft and others 2005) was grown for 7–8 days on solid MS medium without DEX and subsequently transferred to fresh solid or liquid MS medium supplemented with 20 μM DEX and incubated for the indicated time interval while ensuring that the total cultivation interval was 8 days. Steady-state levels of *ipt* transcript were assayed by real-time RT-PCR. Seedlings cultivated for 8 days on MS agar medium without DEX accumulated *ipt* transcript at 1.8% of *ACTIN*, confirming a low level of leakiness in the pOp/LhGR system (Figure 2B). No RT PCR signal was detected in wild type and the parental CaMV35S::LhGR activator line 4c-S5/7 (Craft and others 2005) seedlings (not shown). The basal transcription level did not result in any consistent and significant increase in CK metabolites compared to the wild type, with total CK content amounting to 180 and 150 pmol/g FW for line 11 and wild type, respectively. We next determined the induction kinetics of pOp-ipt/LhGR by determining steady-state levels of *ipt* transcript in seedlings exposed to DEX. As shown in Figure 1B, increased levels of *ipt* transcript were evident within 1 h, and the maximal level of induction corresponding to a 106-fold increase in *ipt* transcript (approaching *ACTIN* transcript levels) was achieved after 6 h of induction by DEX in the liquid medium and subsequently leveled off at 12 and 24 h. Similar induction kinetics were observed when the seedlings were exposed to DEX on MS agar (not shown). Induction in liquid medium was chosen for the subsequent experiments because of the induction kinetics on agar media for short periods (up to 6 h) proved less reproducible, and treatments in liquid medium allowed a more direct comparison with earlier genome-wide analyses of CK action in *Arabidopsis* (Hoth and others 2003; Rashotte and others 2003; Brenner and others 2005). Interestingly, in pOp-ipt/LhGR seedlings germinated and grown for 8 days on an MS medium supplemented with 20 μM dexamethasone, *ipt* transcripts accumulated only at 9.3% of *ACTIN* (Figure 2B).

Morphologic Effects of Cultivation on Medium Supplemented with BA and Continual Induction of *ipt* Gene

No obvious consistent morphologic alterations were observed in pOp^{BK}-ipt line 11 prior to DEX treatment when a small population (approximately 10 individuals)

was inspected. Wild-type and transgenic seedlings growing on MS medium supplemented with BA and DEX, respectively, displayed morphologic alterations typical of CK action, namely, strong inhibition of root development, hypocotyl widening, and reduction of cotyledon area. Accumulation of anthocyanins was apparent in the upper part of hypocotyls, petioles, and partly at the cotyledon margins. Severity of the alterations was dose dependent in seedlings grown on MS medium supplemented with BA. In the transgenic seedlings, phenotype alterations caused by *ipt* activation were less severe than those caused by 2.5 μM BA in the wild-type seedlings (Figure 3).

Dynamics of the CK Pool Upon *ipt* Activation in *Arabidopsis* Seedlings

To investigate dynamics of the CK pool upon *ipt* activation, CK metabolites were analyzed in aliquots of seedlings harvested for *ipt* transcript quantification. Prior to induction, the CK content was comparable in the pOp^{BK}-ipt line 11 and wild type (180 and 150 pmol/g FW, respectively). No significant change in endogenous CK level could be observed after 1 h of DEX treatment. A dramatic increase in *t*-ZMP and a clear accumulation of *t*-Z represented the major alterations in the CK pool after 6 h of DEX treatment. From this time on, conversion to DZMP and other DZ metabolites became apparent and a dramatic increase in conjugation to produce *O*- and *N*-glucosides was observed. After 24 h, levels of all *t*-Z-type CKs were increased dramatically, whereas no significant increase was observed in *c*-Z-type CKs. Although a slight increase in iPMP was observed starting from 6 h of DEX treatment, no major changes were found in iP-type CKs.

To achieve conditions comparable to the long-term treatment with exogenous CKs, the pOp^{BK}-ipt seedlings were grown for 8 days on MS medium supplemented with 20 μM DEX. Real-time RT-PCR analysis revealed steady-state levels of *ipt* transcript amounting to 9.3% of *ACTIN* transcript (Figure 2B). The overall spectrum of CK metabolites was comparable to that found in 8-day-old seedlings treated with DEX for 24 h. However, although the content of free bases remained almost unaltered, phosphates and ribosides were reduced significantly, and a dramatic increase in *N*- and *O*-glucosylated metabolites was observed with the highest preference for *t*-zeatin *N7*-glucoside. Thus, 170 and 195 pmol/FW of bases, 10,340 and 4620 pmol/FW of phosphates, 1425 and 450 pmol/FW of ribosides, 280 and 1610 pmol/FW of *O*-glucosides, 690 and 6280 pmol/FW of *N7*-glucosides, and 185 and 1370 pmol/FW of *N9*-glucosides were found in the seedlings following 24-h and 8-day DEX induction, respectively (see Figures 4 and 5).

Analysis of endogenous CK pools in the seedlings grown in the presence of BA as well as those treated for 1–24 h with BA could not detect any significant alterations in isoprenoid-type CKs (not shown). Thus, the morphological and molecular alterations in BA-treated seedlings can be attributed solely to BA action.

Effects of Increased Levels of Endogenous CKs on the Expression of *AHP* Genes

To compare effects of BA treatment and increase in endogenous CK levels on *AHP* gene expression, we analyzed steady-state levels of the *AHP* transcripts following short- and long-term activation of *ipt* transcription (see

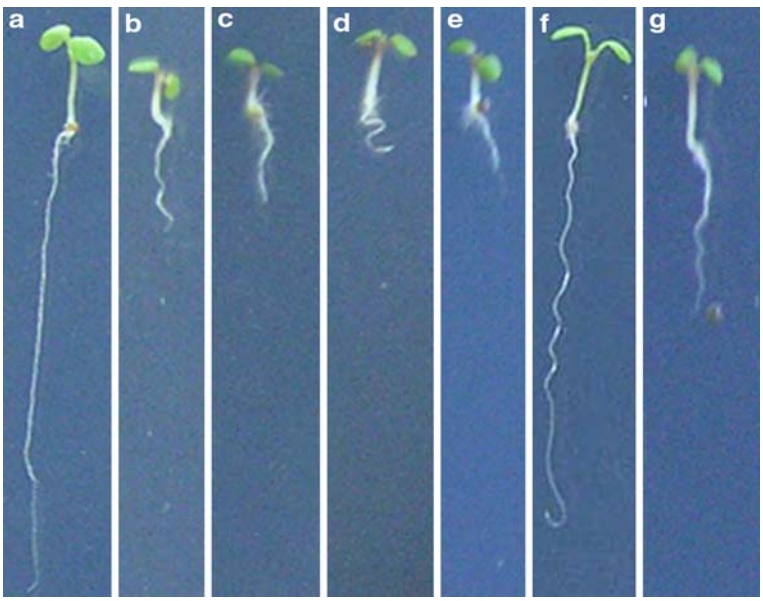

Fig. 3 Seedling morphology in response to long-term CK action. Wild-type seedlings were grown on MS medium (a) supplemented with 2.5 (b), 5.0 (c), 7.5 (d), and 10 (e) μM BA for 8 days. Seedlings of pOp^{BK}-ipt line 11 were grown on MS medium (f) supplemented with 20 μM DEX (g) for 8 days

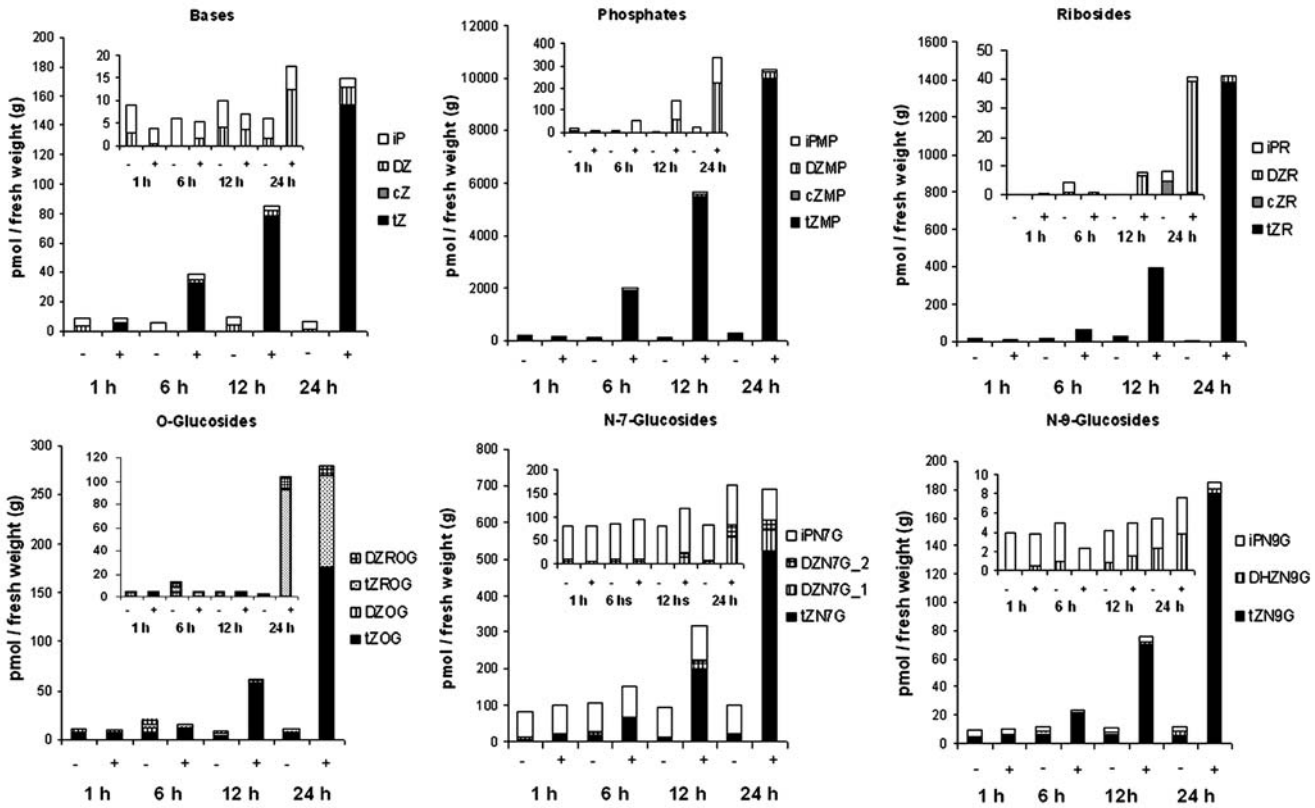

Fig. 4 Dynamics of the CK pool upon induction of *ipt* expression. Seedlings (pOp^{BK}-ipt line 11) were treated with 20 μM DEX in liquid MS medium for the indicated periods and CK metabolites determined by LC-MS/MS. Metabolites not shown were below the detection limit. + and – represent DEX-treated and nontreated seedlings, respectively. Three independent experiments displayed similar trends in CK metabolites, and results of a representative one are presented. Abbreviations: *c*-Z, *cis*-zeatin; *c*-ZR, *cis*-zeatin 9-riboside; *c*-ZMP, *cis*-zeatin 9-riboside-5′-monophosphate; DZ, dihydrozeatin; DZN7G, dihydrozeatin *N7*-glucoside (DZN7G_1 and DZN7G_2 represent enantiomers of DZN7G that are separated under HPLC conditions used; assignment of handedness is not possible as only racemate is available as a standard); DZN9G, dihydrozeatin *N9*-glucoside; DZOG, dihydrozeatin *O*-glucoside; DZR, dihydrozeatin 9-riboside; DZROG, dihydrozeatin 9-riboside *O*-glucoside; DZMP, dihydrozeatin 9-riboside-5′-monophosphate; iP, N^6-(Δ^2-isopentenyl)adenine; iPN7G, N^6-(Δ^2-isopentenyl)adenine *N7*-glucoside; iPN9G, N^6-(Δ^2-isopentenyl)adenine *N9*-glucoside; iPR, N^6-(Δ^2-isopentenyl)adenine 9-riboside; iPMP, N^6-(Δ^2-isopentenyl)adenine 9-riboside-5′-monophosphate; *t*-Z, *trans*-zeatin; *t*-ZN7G, *trans*-zeatin *N7*-glucoside; *t*-ZN9G, *trans*-zeatin *N9*-glucoside; *t*-ZOG, *trans*-zeatin *O*-glucoside; *t*-ZR, *trans*-zeatin 9-riboside; *t*-ZROG, *trans*-zeatin 9-riboside *O*-glucoside; *t*-ZMP, *trans*-zeatin 9-riboside-5′-monophosphate

above). The general pattern of *AHP* gene expression following the short-term *ipt* activation resembled the one found in response to the short-term BA treatment except that the maximal steady-state transcript levels were higher and were reached after only 12 h of *ipt* activation (Figure 1A). Surprisingly, no statistically significant increase in *AHP* transcript steady-state levels was found in response to long-term *ipt* activation (Figure 2B).

Type-B ARR-Binding Sites in the Upstream Regions of *AHP* Genes

Type-B ARRs have been implicated in transcriptional elevation of the type-A *ARR*s in response to CK. The common-binding motif (A/T)GAT(A/T) of the type-B ARRs (Lohrmann and Harter 2002 and references therein) and the special-binding motif GGATT of ARR11 (Imamura and others 2003) were found within 1 kb upstream of the translational start site of *AHP* genes as follows: *AHP1*: 1× AGATA, 5× TGATA, 2× TGATT, and 3× GGATT; *AHP2*: 1× AGATT and 3× GGATT; *AHP3*: 2× AGATT, 1× TGATT, and 2× GGATT; *AHP4*: 1× AGATA, 1× AGATT, 2× TGATA, 1× TGATT; *AHP5*: 1× AGATA, 1× AGATT, 1× TGATA, 1× TGATT, and 2 × GGATT (Figure 6). Their frequency was higher compared to random occurrence, especially for *AHP1*. Except for *AHP4*, the highest increase over random occurrence was found for the special-binding motif GGATT. Based on the actual GC content found within 1 kb upstream of the translational start site of *AHP* genes, GGATT should randomly occur 0.6 times (compared to the actual 3 times found) in *AHP1*,

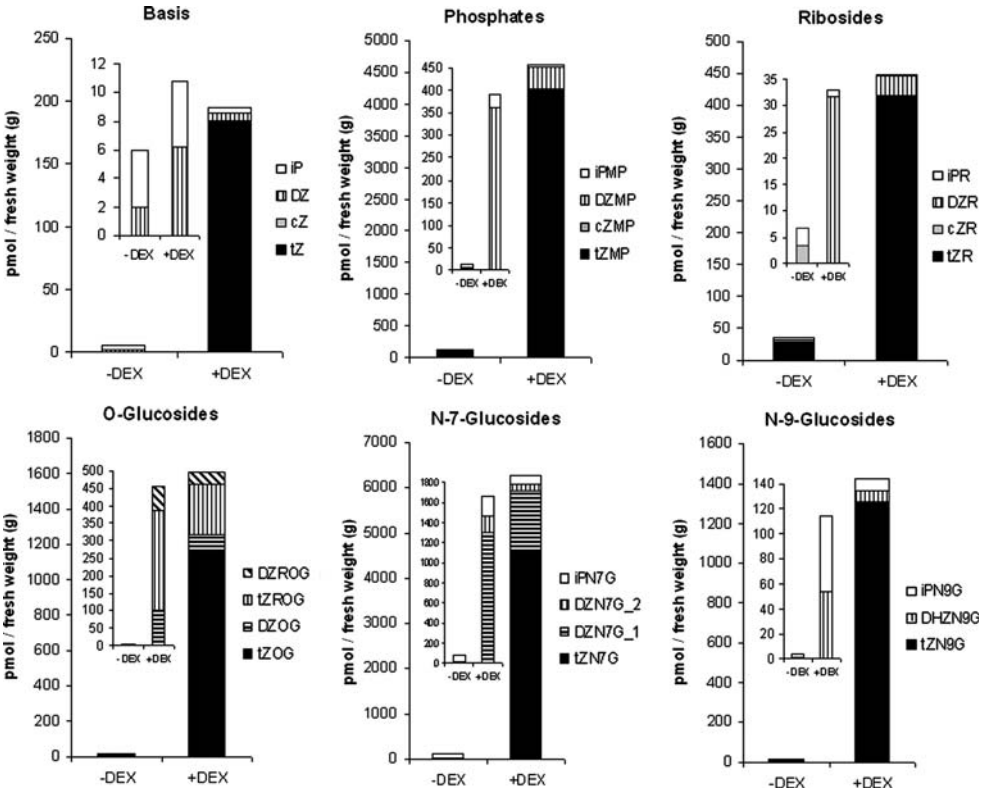

Fig. 5 CK pool in seedlings with continuously activated expression of *ipt*. Seedlings (pOp^{BK}-ipt line 11) were germinated and grown on MS plates supplemented with 20 μM DEX for 8 days and CK metabolites determined by LC-MS/MS. Metabolites not shown were below the detection limit. Three independent experiments displayed similar trends in CK metabolites, and results of a representative one are presented. For abbreviations see Figure 4

0.7 times (compared to 2 times found) in *AHP2*, 0.9 times (compared to 2 times found) in *AHP3*, and 1.2 times (compared to 2 times found) in *AHP5*. For comparison, frequency of random occurrence was calculated in the same way for the 1-kb-upstream untranslated region and compared to the actually found number of GGATT motifs in the same region in several selected genes. The frequency of the special-binding motif was also increased in type-A *ARR* genes—expected random occurrence 0.6 compared to 1 time found in *ARR5*, expected random occurrence 0.8 compared to 2 times found in *ARR7*, and random occurrence 0.8 compared to 1 time found in *ARR16*. In contrast, type-B *ARR* genes *ARR2* and *ARR10* lack the GGATT motif, although the calculated random occurrence is 0.5 and 1.3 times, respectively. The frequency of the GGATT motif was underrepresented or comparable to calculated random occurrence in CK downregulated genes—found 1 time compared to random occurrence of 1 time in a gene encoding E3 ubiquitin ligase, found 2 times compared to random occurrence of 1.9 times in *AHP6*, and absent compared to random occurrence of 1.5 times in the *ARGONAUTE* gene. The GGATT motif was absent in the 1-kb-upstream untranslated regions of genes that have no apparent relation to CK response/signaling, *SAG12* and *UBQ10*, although in the same region of these genes it should randomly occur 0.8 times. Thus, the GGATT motif is apparently enriched in genes positively regulated by CKs; this remains true also for the common-binding motif (A/T)GAT(A/T). The per-gene sum of the frequencies of all these motifs found in the 1-kb-upstream untranslated region gene is on average about two to three times higher in type-A *ARR* genes compared to *AHP* genes (not shown), consistent with a higher level of induction of the former by CKs. The frequency of these motifs in the upstream region of *AHP5* might indicate its regulation by CKs at developmental stages not investigated in this study.

Discussion

We analyzed the effects of CK treatment and increased endogenous CK levels on the expression of the individual members of a gene family coding for AHPs, histidine-containing phosphotransmitters, in *Arabidopsis*. The binary pOp-ipt/LhGR system of regulatable gene expression was employed to increase endogenous CK levels. Following *ipt* activation, a rapid and highly preferential increase in *t*-Z-type CKs was observed, whereas other types of CKs showed no or only marginal increases. The levels of *t*-ZMP, *t*-ZR, and *t*-Z under long-term *ipt* activation suggest that the seedlings, in contrast to older plants, may have as-yet unrecognized difficulties in efficiently downregulating active forms of the hormone. Using real-time RT-PCR, transient increases in steady-state levels of *AHP1-4* transcripts in response to both the short-term aromatic CK treatment and the increase in endogenous *t*-Z-type CK

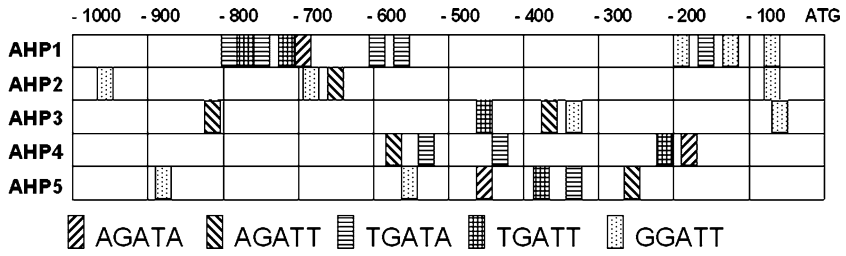

Fig. 6 Putative *cis*-acting motifs in the promoters of *AHP* genes. The DNA sequences 1000 bp upstream of the predicted translational start site of the *AHP* genes were analyzed for the *cis*-acting sequence motifs that represent potential sites of CK regulation. The positions of the common-binding motif (A/T)GAT(A/T) of type-B ARRs and the special-binding motif GGATT of ARR11 are depicted by boxes as indicated

levels was found, although *AHP5* transcripts remained unaltered. Surprisingly, the increase in steady-state levels of *AHP1-4* transcripts observed in seedlings cultivated continuously in the presence of exogenous aromatic CK was not paralleled in seedlings with constitutively increased endogenous *t*-Z-type CKs.

The Binary pOp/LhGR System to Drive *ipt* Expression in *Arabidopsis*

The pOp/LhGR dexamethasone-inducible system has been used in *Arabidopsis* and tobacco to regulate the expression of *uidA* and *ipt* genes. The system exhibited stringent regulation and strong induced phenotypes in soil and tissue culture as judged by GUS activity and phenotype analysis of the *uidA* and *ipt* expressing plants, respectively (Craft and others 2005; Šámalová and others 2005). We extended the previous analysis of *ipt*-expressing plants by reliable quantification of steady-state levels of *ipt* transcripts in noninduced *Arabidopsis* seedlings and during the course of induction and correlated them with the dynamics of the total CK pool. The level of *ipt* transcript found in noninduced seedlings (1.8% of the *ACTIN* transcript) represents the first quantitative estimation of leakiness in the pOp/LhGR system at the transcript level. The highest level of *ipt* transcript was observed at 6 h of induction and represented a 106-fold increase compared to the noninduced state and approached the steady-state level of *ACTIN* transcripts. The noninduced level of transcript did not result in any consistent increase in CK levels as determined by LC-MS/MS analysis, indicating that reaching a threshold *ipt* transcript level higher than 1.8% of *ACTIN* transcript might be necessary to achieve sufficient ipt enzymatic activity to perturb steady-state levels of CK metabolites found in wild-type *Arabidopsis* seedlings. Upon *ipt* induction, a sharp increase in CK levels was observed, amounting to 13,089 pmol/g FW total CK after 24 h of DEX treatment compared to 180 pmol/g FW found in untreated seedlings. Efficiency of transcriptional control imposed upon *ipt* in the pOp-ipt/LhGR system cannot be compared directly with the previously described systems of regulated *ipt* expression because no attempt to quantify *ipt* transcript levels in those systems has been published. When total CK levels found upon *ipt* induction are chosen as an indirect measure of performance, the pOp-ipt/LhGR system appears the most efficient out of the currently available systems of regulated *ipt* expression. Thus, total CK levels of 58, 2500, and 3000 pmol/g FW were found 8 h after a single heat shock treatment in HSIPT *Arabidopsis* seedlings (Rupp and others 1999), 12 h of DEX treatment in *ipt* transgenic *Arabidopsis* seedlings (Åstot and others 2000), and 24 h of chlortetracycline treatment in detached leaves of tet-ipt tobacco (Redig and others 1996), respectively. For comparison, total CK levels of 2273, 6578, and 13089 pmol/g FW were found in the pOp^{BK}-ipt line11 after 6, 12, and 24 h of DEX induction, respectively. However, it should be noted that the comparison is based on the analysis of one or two lines in each case, which are assumed to offer the best induction ratios for each system, and a more comprehensive analysis is hampered by tedious CK analysis.

Interestingly, in *Arabidopsis* seedlings growing on plates supplemented with DEX for 8 days, steady-state levels of *ipt* transcript were found to be as low as 9.3% of *ACTIN* compared to about 108% of *ACTIN* observed 6 h after DEX application to 8-day-old seedlings. This is consistent with *uidA* transcripts remaining stable for only about 4 days when pOpOff2(hyg)::PDS seedlings were kept continuously on DEX-supplemented MS medium as determined by Northern blot analysis, which is generally less sensitive compared to real-time RT-PCR (Wielopolska and others 2005).

Dynamics of CK Metabolism in Response to *ipt* Activation in *Arabidopsis*

We employed an *A. tumefaciens ipt* gene as the only currently available molecular tool to achieve a specific increase in *t*-Z type CKs to investigate regulation of expression in the *AHP* gene family specifically by *t*-Z-type

CKs. Although *t*-Z-type CKs constitute an important part of the CK pool in all plants investigated, including *Arabidopsis*, all genuine plant IPTs characterized up to now preferentially increase iP-type CKs when expressed in transgenic plants (Zubko and others 2002; Sun and others 2003; Sakakibara and others 2005). The dynamics of the CK metabolite pool following induction of *ipt* expression have been partly characterized in *Arabidopsis* seedlings harboring the *ipt* gene under the transcriptional control of the *hsp70* promoter of *Drosophila melanogaster* (Rupp and others 1999; Werner and others 2003). The dynamics of the CK metabolite pool found in the current study are fully consistent with the so-called alternative iPMP-independent pathway, being the major although not the exclusive biosynthetic pathway for *t*-Z-type CKs in *ipt*-expressing *Arabidopsis* in that a steep increase in *t*-ZMP and only a marginal increase in iPMP are observed following *ipt* activation (Åstot and others 2000). However, the marginal increase in iPMP steady-state level might be expected for the iPMP-dependent pathway as a major route contributing to the *t*-Z-type CK pool under special circumstances, that is, when the rate of iPMP hydroxylation approaches the rate of iPMP biosynthesis. Although this special situation is quite unlikely considering the enormous rate of *ipt* expression driven by the pOp/LhGR system that should be matched by an almost equal increase in the activity of the endogenous CK hydroxylases CYP735A1 and CYP735A2, it cannot be excluded based solely on our data. Rather, label-tracing experiments would be necessary to determine the relative contributions of iPMP-independent and iPMP-dependent pathways to the *t*-Z-type CK pool. The kinetics of the increase in *t*-ZR and *t*-Z are consistent with their formation mainly from *t*-ZMP (Sakakibara and others 2005). A detailed analysis of the effect of the CK metabolite pool dynamics upon *ipt* activation enabled us to get a better insight into the extent of metabolic conversions available in *Arabidopsis* seedlings to maintain homeostasis of this physiologically important type of CKs. Thus, all activities leading to conversions of *t*-Z, *t*-ZR, and *t*-ZMP, except the one from *t*-Z to *c*-Z, are apparent from the kinetics of increases in the individual metabolites. The reduction of *t*-Z to the DZ side chain likely at the nucleotide level might be assumed based on the finding that DZMP is the first to rise and is the most abundant DZ-type CK (Figure 4). Following increases in free bases and concomitantly increases in ribosides, the corresponding *N*- and *O*-glucosides started to accumulate. The nature of the glucosides indicates that all possible glucosylation reactions take place at high levels in *Arabidopsis* seedlings, with a preference for *N7*-glucosylation. However, very low if any increases in iPN7G and iPN9G suggest either that iPMP undergoes rapid hydroxylation to *t*-ZMP, or iPR and iP are degraded with high efficiency by CK oxidase/dehydrogenase. Thus, our results extend previous findings on CK metabolism in *Arabidopsis* in that they (1) conclusively establish *N7*-glucosylation as the major inactivating conjugation reaction for CKs, (2) demonstrate a significant extent of reversible CK inactivation via *O*-glucosylation, (3) show significant conversion of *t*-Z to DZ occurring probably at the nucleotide level, and (4) indicate the absence of interconversions between *t*-Z- and *c*-Z-type CK pools in the early stages of seedling development. In the future, labeling experiments might contribute to a deeper understanding of the individual steps in CK metabolism and their interconnection. Interestingly, the high levels of *t*-Z, *t*-ZR, and *t*-ZMP (as well as those of CK *O*- and *N*-glucosides) found in 8-day-old seedlings with constitutively induced *ipt* expression suggest that young seedlings—as opposed to older plants (for example, Werner and others 2003)—have as-yet unrecognized difficulties in efficiently downregulating active CK metabolites or those that could readily become active. However, the actual rate of IPT activity was determined in neither the young seedlings nor the older plants. Thus, it remains to be determined rigorously whether a potentially lower actual input into a CK pool in older plants cannot account for the difference.

Regulation of Gene Expression in *AHP* Gene Family by CKs

Based on Northern blot analysis and genome-wide expression profiling of CK action, previous reports have concluded that CKs do not affect the expression level of *AHP* genes (Suzuki and others 2000; Rashotte and others 2003; Brenner and others 2005) except *AHP5* which is induced under specific conditions (Hoth and others 2003). Here we report, for the first time to our knowledge, that short-term BA treatment of and *ipt* gene induction in *Arabidopsis* seedlings resulted in a transient increase in steady-state levels of *AHP1*, *AHP2*, *AHP3*, and *AHP4* transcripts whose maximal level of induction (2-3-fold) was reached at 6 and 12 h, respectively, whereas the *AHP5* gene was CK insensitive. The delay in reaching maximal transcript levels of *AHP1-4* in the course of *ipt* activation correlates well with the time needed for the increase in endogenous CK levels following increases in *ipt* transcript levels. A partial desensitization of the response pathway after prolonged exposure to CKs might explain this expression pattern. Previous works reported transient regulation of transcripts involved in CK signaling, including several type-A *ARRs* (D'Agostino and others 2000; Hoth and others 2003) and *CRE1* (Hoth and others 2003). In *Arabidopsis* seedlings, genome-wide analysis of gene expression in response to increased CK levels revealed that

39% of transcripts induced after 15 min returned to their basal levels after 120 min of CK treatment (Brenner and others 2005), and almost 50% of transcripts induced after 6 h returned to their basal levels after 24 h of *ipt* induction (Hoth and others 2003). Thus, the transient transcript kinetics upon induction of gene expression by CKs appears to be a widespread phenomenon. In the genome-wide expression profiling of CK action, a 1.8-, 2-, and 3-fold change in expression level compared with the control was chosen as a minimum for a gene to be called altered in response to CK (Brenner and others 2005; Rashotte and others 2003; and Hoth and others 2003, respectively); thus, the extent of induction of *AHP* genes is at or just below the chosen cutoff levels. Careful inspection of the expression data identifies signs of transient induction of *AHP1*, *AHP2*, and *AHP3* peaking at 8 h of BA treatment. Nevertheless, the *AHP* genes were scored as CK insensitive as the degree of induction remained below twofold (Rashotte and others 2003). An almost 2- and 1.4-fold transient increase in *AHP4* and *AHP1* transcript levels, respectively, following *ipt* induction was not scored as significant by Hoth and others (2003) because it remained below the cutoff level of a threefold increase. Thus, sensitivity and accuracy of real-time RT-PCR enabled us to detect upregulation by CKs of *AHP1*, *AHP2*, *AHP3*, and *AHP4* genes that remained unrecognized in the previous genome-wide analyses. Differences in the CK response were observed in *AHP5*, whose transcripts were upregulated in 2-week-old seedlings following *ipt* gene activation (Hoth and others 2003) but were not affected by CK treatment and *ipt* gene induction in 8-day-old seedlings in our experiments. Apparently regulation of *AHP* genes may vary during seedling development. The upregulation by CKs is consistent with the identification of type-B ARR-binding sites in the upstream regions of *AHP1-5* genes (Figure 6). A core sequence motif GATCTT that closely matches the binding sites for type-B *ARR*s was found, in addition to promoters of primary response type-A *ARR* genes, in putative promoter regions of other CK-responsive genes whose induction was observed within a broad time window ranging from 45 min to 24 h. Rashotte and others (2003) correlated the frequency of this common sequence motif in the upstream promoter regions with the level rather than the kinetics of induction of the corresponding genes. Thus, the presence of type-B ARR-binding sites in the upstream regions of *AHP1-5* genes reported in this study is consistent with the previous finding that type-B ARR-binding sites are not restricted to promoter regions of CK primary response genes but rather might indicate a general responsiveness to CKs.

Dramatic differences were observed when *AHP* transcript levels were compared in seedlings (1) exposed to long-term BA treatment and (2) expressing the *ipt* gene for an extended period of time. Although all *AHP* transcripts except *AHP5* were elevated in a dose-dependent manner in seedlings grown in the presence of BA, no statistically significant changes in *AHP* transcripts were found in response to the long-term *ipt* activation. At the same time, the level of *t*-ZMP, the most abundant *t*-Z-type CK directly activating the CK receptor AHK3 (Spíchal and others 2004), was greater than 4 nmol/g FW (Figure 5), roughly corresponding to 5 μM solution assuming 80% water content of the seedlings. At this concentration, exogenously applied BA caused between half to maximal or almost maximal activation in *AHP1-4* genes (Figure 2). Thus, *t*-Z-type CKs apparently induce only a transient increase in *AHP* transcript levels, whereas BA might function in a biphasic manner, first inducing the transient spurt and later a sustained increase in *AHP* transcript levels. Distinct effects of short- and long-term CK exposures were reported in tobacco seedlings (Lexa and others 2002). Based on ligand specificity analyses of CK receptors in *Arabidopsis*, specific functions were inferred for diverse types of CKs (Spíchal and others 2004). Effects on gene expression of BA and *t*-Z treatments were compared in *Arabidopsis* seedlings (Rashotte and others 2003). Although both CKs caused upregulation of an almost identical set of genes, fewer genes were downregulated by *t*-Z compared to BA, which suggests that some of these genes may be specifically downregulated by BA. Future analysis of this and similar distinct effects of different types of CKs at the molecular level might be expected to shed new light on the hypothesized distinct roles of individual CK types. However, to allow for unequivocal interpretations, the design of future *in planta* experiments has to take into account differences in metabolic inactivation and potential differences in subcellular compartmentation of the individual CKs. Furthermore, when compared to the effects of expressing *ipt* for an extended period, long-term BA treatment resulted in more pronounced morphologic alterations in *Arabidopsis* seedlings. Thus, the possibility cannot be fully excluded that the increased *AHP* transcript levels might be a secondary effect of BA action.

Seedling responses to elevated CK levels were inferred from the nature of the genes affected by CKs and their kinetics of induction (Hoth and others 2003; Rashotte and others 2003). Reduction of both sensitivity of the response pathway and the level of the active hormone might be deduced from expression profiling of CK action. The CK signaling response is desensitized by upregulation of type-A *ARR*s, which act as negative regulators of the CK response pathway (To and others 2004). Expression of the CK receptor *CRE1* was upregulated over time, reaching a maximum at 24 h in response to BA treatment (Rashotte and others 2003), which is similar to the induction of

ethylene receptors by ethylene. In an independent study, *CRE1* was transiently upregulated in response to *ipt* gene activation (Hoth and others 2003). A higher activity of CRE1 may be achieved by activating the transcription of *CRE1*, thus enhancing the reception of the CK signal and corresponding downstream changes in gene expression. Alternatively, the increased *CRE1* transcription may reflect a potential negative-regulator role of CRE1 in the CK response because His kinases in other two-component systems can act as both His kinases and phosphatases (Stock and others 2000). The induction kinetics of *AHP1-4* genes are distinct from that of type-A *ARR* genes. Thus, in contrast to type-A *ARR* genes, they cannot be classified as CK primary response genes. However, their induction kinetics resemble that of *CRE1* found by Hoth and others (2003). Similar to *CRE1*, the transient increase in their transcript levels might implicate their involvement in enhancing CK signal transduction. However, a more intriguing role in two-component signaling might be inferred from the ability of AHP1 and AHP2 to phosphorylate the receiver domain of the histidine kinase CKI1 found in *in vitro* experiments (Nakamura and others 1999). Interestingly, the *Arabidopsis* pseudo-HPt AHP6, which negatively regulates CK signaling by apparently inhibiting phosphotransfer from phosphorylated AHP to ARR, is downregulated by exogenous CK at the transcriptional level (Mähönen and others 2006). This indicates an inverse transcriptional regulation of AHPs that is part of the CK signaling chain and those acting to inhibit CK signaling.

Acknowledgments The authors thank Dr. Ian Moore for assistance in the early stages of this work. They thank Drs. Miroslav Kamínek, Nagavalli S. Kiran, and Markéta Šámalová for critical reading of and valuable discussions on the manuscript. They thank Dr. Hana Konečná and Renata Bendová for synthesizing oligonucleotide primers, Dr. Eva Paděrová for DNA sequencing, Mgr. Přemysl Souček for help with real-time RT-PCR experiments in the initial phase of this project, and Ms. Martina Válková for help with extraction and purification of cytokinins. This work was supported by grants LN00A081, MSM0021622415, 1M06030, and LC06034 (Ministry of Education of the Czech Republic), AVOZ50040507 (Academy of Sciences of the Czech Republic), IAA600380507 and IAA600040612 (Grant Agency of the Academy of Sciences of the Czech Republic), and a Royal Society Joint Project Grant (rc/jp/jun98) to Ian Moore and BB.

References

Akiyoshi DE, Klee H, Amasino RM, Nester EW, Gordon MP (1984) T-DNA of *Agrobacterium tumefaciens* encodes an enzyme of cytokinin biosynthesis. Proc Natl Acad Sci U S A 81:5994–5998

An YQ, McDowell JM, Huang S, McKinney EC, Chambliss S, Meagher RB (1996) Strong, constitutive expression of the *Arabidopsis* ACT2/ACT8 actin subclass in vegetative tissues. Plant J 10:107–121

Åstot C, Doležal K, Nordström A, Wang Q, Kunkel T, Moritz T, Chua N-H, Sandberg G (2000) An alternative cytokinin biosynthesis pathway. Proc Natl Acad Sci U S A 97:14778–14783

Barry GF, Rogers SG, Fraley RT, Brand L (1984) Identification of a cloned cytokinin biosynthetic gene. Proc Natl Acad Sci U S A 81:4776–4780

Bielski RL (1964) The problem of halting enzyme action when extracting plant tissues. Anal Biochem 121:431–442

Binns AN (1994) Cytokinin accumulation and action: biochemical, genetic and molecular approaches. Annu Rev Plant Physiol Plant Mol Biol 45:173–196

Brandstatter IB, Kieber JJ (1998) Two genes with similarity to bacterial response regulators are rapidly and specifically induced by cytokinin in *Arabidopsis*. Plant Cell 10:1009–1019

Brenner WG, Romanov GA, Kollmer I, Burkle L, Schmulling T (2005) Immediate-early and delayed cytokinin response genes of *Arabidopsis thaliana* identified by genome-wide expression profiling reveal novel cytokinin-sensitive processes and suggest cytokinin action through transcriptional cascades. Plant J 44:314–333

Brzobohatý B, Moore I, Kristoffersen P, Bako L, Campos N, Schell J, Palme K (1993) Release of active cytokinin by a β-glucosidase localized to the maize root meristem. Science 262:1051–1054

Brzobohatý B, Moore I, Palme K (1994) Cytokinin metabolism: implications for regulation of plant growth and development. Plant Mol Biol 26: 1483–1497

Craft J, Šámalová M, Baroux C, Townley H, Martinez A, Jepson I, Tsiantis M, Moore I (2005) New pOp/LhG4 vectors for stringent glucocorticoid-dependent transgene expression in *Arabidopsis*. Plant J 41:899–918

D'Agostino IB, Deruere J, Kieber JJ (2000) Characterization of the response of the *Arabidopsis* response regulator gene family to cytokinin. Plant Physiol 124:1706–1717

Dobrev PI, Kaminek M (2002) Fast and efficient separation of cytokinins from auxin and abscisic acid and their purification using mixed-mode solid-phase extraction. J Chromatogr A 121:431–442

Grefen C, Harter K (2004) Plant two-component systems: principles, functions, complexity and cross talk. Planta 219:733–742

Haberer G, Kieber JJ (2001) Cytokinins: new insights into a classic phytohormone. Plant Physiol 128:354–362

Hoth S, Ikeda Y, Morgante M, Wang X, Zuo J, Hanafey MK, Gaasterland T, Tingey SV, Chua N-H (2003) Monitoring genome-wide changes in gene expression in response to endogenous cytokinin reveals targets in *Arabidopsis thaliana*. FEBS Lett 554:373–380

Hou B, Lim E-K, Higgins GS, Bowles DJ (2004) N-glucosylation of cytokinins by glycosyltransferases of *Arabidopsis thaliana*. J Biol Chem 279:47822–47832

Houba-Hérin N, Pethe C, d'Alayer J, Laloue M (1999) Cytokinin oxidase from *Zea mays*: purification, cDNA cloning and expression in moss protoplasts. Plant J 17:615–626

Hradilová J, Brzobohatý B (2007) Expression pattern of the *AHP* gene family from *Arabidopsis thaliana* and organ specific alternative splicing in the *AHP5* gene. Biol Plantarum 51:257–267

Hutchison CE, Kieber JJ (2002) Cytokinin signaling in *Arabidopsis*. Plant Cell 14:47–59

Hwang I, Sheen J (2001) Two-component circuitry in *Arabidopsis* cytokinin signal transduction. Nature 413:383–389

Imamura A, Hanaki N, Nakamura A, Suzuki T, Tanaguchi M, Kiba T, Ueguchi C, Sugiyama T, Mizuno T (1999) Compilation and characterization of *Arabidopsis thaliana* response regulators implicated in His-Asp phosphorelay signal transduction. Plant Cell Physiol 40:733–742

Imamura A, Yoshino Y, Mizuno T (2001) Cellular localization of the signaling components of *Arabidopsis* His-to-Asp phosphorelay. Biosci Biotechnol Biochem 65:2113–2117

Imamura A, Kiba T, Tajima Y, Yamashino T, Mizuno T (2003) In vivo and in vitro characterization of the ARR11 response

regulator implicated in the His-to-Asp phosphorelay signal transduction in *Arabidopsis thaliana*. Plant Cell Physiol 44:122–131

Inoue T, Higuchi M, Hashimoto Y, Seki M, Kobayashi M, Kato T, Tabata S, Shinozaki K, Kakimoto T (2001) Identification of CRE1 as a cytokinin receptor from *Arabidopsis*. Nature 409:1060–1063

Kakimoto T (1996) CKI1, a histidine kinase homolog implicated in cytokinin signal transduction. Science 274:982–985

Kakimoto T (2001) Identification of plant cytokinin biosynthetic enzymes as dimethylallyl diphosphate:ATP/ADP isopentenyltransferases. Plant Cell Physiol 42:677–685

Kiran NS, Polanská L, Fohlerová R, Mazura P, Válková M, Šmeral M, Zouhar J, Malbeck J, Dobrev IP, Macháčková I, Brzobohatý B (2006) Ectopic over-expression of the maize β-glucosidase Zm-p60.1 perturbs cytokinin homeostasis in transgenic tobacco. J Exp Bot 57:985–996

Lexa M, Genkov TN, Brzobohatý B (2002) Inhibitory effects of elevated endogenous cytokinins on nitrate reductase in ipt-expressing tobacco are eliminated by short-term exposure to benzyladenine. Physiol Plant 115:284–290

Lexa M, Genkov TN, Malbeck J, Macháčková I, Brzobohatý B (2003) Dynamics of endogenous cytokinin pools in tobacco seedlings: A modeling approach. Ann Bot (Lond) 91:585–597

Lohrmann J, Harter K (2002) Plant two-component signaling systems and the role of response regulators. Plant Physiol 128:363–369

Mähönen AP, Bishopp A, Higuchi M, Nieminen KM, Kinoshita K, Törmäkangas K, Ikeda Y, Oka A, Kakimoto T, Helariutta Y (2006) Cytokinin signaling and its inhibitor AHP6 regulate cell fate during vascular development. Science 311:94–98

Martin RC, Mok MC, Mok DWS (1999a) Isolation of a cytokinin gene, *ZOG1*, encoding zeatin O-glucosyltransferase of *Phaseolus lunatus*. Proc Natl Acad Sci U S A 96:284–289

Martin RC, Mok MC, Mok DWS (1999b) A gene encoding the cytokinin enzyme zeatin O-xylosyltransferase of *Phaseolus vulgaris*. Plant Physiol 120:553–557

Martin RC, Mok DWS, Smets R, Van Onckelen HA, Mok MC (2001) Development of transgenic tobacco harbouring a zeatin O-glucosyltransferase gene from *Phaseolus*. In Vitro Cell Dev Biol 37:354–360

Miyata S, Urao T, Yamaguchi-Shinozaki K, Shinozaki K (1998) Characterization of genes for two-component phosphorelay mediators with a single HPt domain in *Arabidopsis thaliana*. FEBS Lett 437:11–14

Mok DW, Mok MC (2001) Cytokinin metabolism and action. Annu Rev Plant Physiol Plant Mol Biol 89:89–118

Morris RO, Bilyeu KD, Laskey JG, Cheikh NN (1999) Isolation of a gene encoding a glycosylated cytokinin oxidase from maize. Biochem Biophys Res Commun 255:328–333

Nakamura A, Kakimoto T, Imamura A, Suzuki T, Ueguchi C, Mizuno T (1999) Biochemical characterization of a putative cytokinin-responsive his-kinase, CKI1, from *Arabidopsis thaliana*. Biosci Biotechnol Biochem 63:1627–1630

Papon N, Vansiri A, Gantet P, Chénieux J-C, Rideau M, Crèche J (2004) Histidine-containing phosphotransfer domain extinction by RNA interference turns off a cytokinin signaling circuitry in *Catharanthus roseus* suspension cells. FEBS Lett 558:85–88

Rashotte AM, Carson SDB, To JPC, Kieber JJ (2003) Expression profiling of cytokinin action in *Arabidopsis*. Plant Physiol 132:1998–2011

Redig P, Schmülling T, Van Onckelen H (1996) Analysis of cytokinin metabolism in ipt transgenic tobacco by liquid chromatography-tandem mass spectrometry. Plant Physiol 112:141–148

Rupp H-M, Frank M, Werner T, Strnad M, Schmülling T (1999) Increased steady state mRNA levels of the STM and KNAT1 homeobox genes in cytokinin overproducing *Arabidopsis thaliana* indicate a role for cytokinins in the shoot apical meristem. Plant J 18:557–563

Sáenz L, Jones LH, Oropeza C, Vláčil D, Strnad M (2003) Endogenous isoprenoid and aromatic cytokinins in different plant parts of *Cocos nucifera* (L.). Plant Growth Regul 39:205–215

Sakai H, Aoyama T, Oka A (2000) *Arabidopsis* ARR1 and ARR2 response regulators operate as transcription activators. Plant J 24:703–711

Sakakibara H, Kasahara H, Ueda N, Kojima M, Takei K, Hishiyama S, Asami T, Okada K, Kamiya Y, Yamaya T, Yamaguchi S (2005) *Agrobacterium tumefaciens* increases cytokinin production in plastids by modifying the biosynthetic pathway in the host plant. Proc Natl Acad Sci U S A 102:9972–9977

Šámalová M, Brzobohatý B, Moore I (2005) pOp6/LhGR: a stringently regulated and highly responsive dexamethasone-inducible gene expression system for tobacco. Plant J 41:919–935

Spíchal L, Rakova NY, Riefler M, Mizuno T, Romanov G, Strnad M, Schmülling T (2004) Two cytokinin receptors of *Arabidopsis thaliana*, CRE1/AHK4 and AHK3, differ in their ligand specificity in a bacterial assay. Plant Cell Physiol 45:1299–1305

Stock AM, Robinson VL, Goudreau PN (2000) Two-component signal transduction. Annu Rev Biochem 69:183–215

Strnad M (1997) The aromatic cytokinins. Physiol Plant 101:674–688

Sun J, Niu Q-W, Tarkowski P, Zheng B, Tarkowska D, Sandberg G, Chua N-H, Zuo J (2003) The *Arabidopsis* AtIPT8/PGA22 gene encodes an isopentenyl transferase that is involved in de novo cytokinin biosynthesis. Plant Physiol 131:167–176

Suzuki T, Imamura A, Ueguchi C, Mizuno T (1998) Histidine-containing phosphotransfer (HPt) signal transducers implicated in His-to-Asp phosphorelay in *Arabidopsis*. Plant Cell Physiol 39:1258–1268

Suzuki T, Sakurai K, Imamura A, Nakamura A, Ueguchi C, Mizuno T (2000) Compilation and characterization of histidine-containing phosphotransmitters implicated in His-to-Asp phosphorelay in plants: AHP signal transducers of *Arabidopsis thaliana*. Biosci Biotechnol Biochem 6:2486–2489

Suzuki T, Miwa K, Ishikawa K, Yamada H, Aiba H, Mizuno T (2001a) The *Arabidopsis* sensor His-kinase, AHK4, can respond to cytokinins. Plant Cell Physiol 42:107–113

Suzuki T, Sakurai K, Ueguchi C, Mizuno T (2001b) Two types of putative nuclear factors that physically interact with histidine-containing phosphotransfer (Hpt) domains, signaling mediators in His-to-Asp phosphorelay, in *Arabidopsis thaliana*. Plant Cell Physiol 42:37–45

Suzuki T, Ishikawa K, Yamashino T, Mizuno T (2002) An *Arabidopsis* histidine-containing phosphotransfer (HPt) factor implicated in phosphorelay signal transduction: Overexpression of AHP2 in plants results in hypersensitiveness to cytokinin. Plant Cell Physiol 43:123–129

Szyroki A, Ivashikina N, Dietrich P, Roelfsema MR, Ache P, Reintanz B, Deeken R, Godde M, Felle H, Steinmeyer R, Palme K, Hedrich R (2001) KAT1 is not essential for stomatal opening. Proc Natl Acad Sci U S A 98:2917–2921

Takei K, Sakakibara H, Sugiyama T (2001) Identification of genes encoding adenylate isopentenyltransferase, a cytokinin biosynthesis enzyme, in *Arabidopsis thaliana*. J Biol Chem 276:26405–26410

Takei K, Yamaya T, Sakakibara H (2004) *Arabidopsis CYP735A1* and *CYP735A2* encode cytokinin hydroxylases that catalyze the biosynthesis of *trans*-zeatin. J Biol Chem 279:41866–41872

Tanaka Y, Suzuki T, Yamashino T, Mizuno T (2004) Comparative studies of the AHP histidine-containing phosphotransmitters implicated in His-to-Asp phosphorelay in *Arabidopsis thaliana*. Biosci Biotechnol Biochem 68:462–465

To JP, Haberer G, Ferreira FJ, Deruere J, Mason MG, Schaller GE, Alonso JM, Ecker JR, Kieber JJ (2004) Type-A *Arabidopsis* response regulators are partially redundant negative regulators of cytokinin signaling. Plant Cell 16:658–671

Ueguchi C, Sato S, Kato T, Tabata S (2001) The AHK4 gene involved in the cytokinin-signalling pathway as a direct receptor molecule in *Arabidopsis thaliana*. Plant Cell Physiol 42:751–755

Werner T, Motyka V, Laucou V, Smets R, Van Onckelen H, Schmülling T (2003) Cytokinin-deficient transgenic *Arabidopsis* plants show multiple developmental alterations indicating opposite functions of cytokinins in the regulation of shoot and root meristem activity. Plant Cell 15:2532–2550

Wielopolska A, Townley H, Moore I, Waterhouse P, Helliwell C (2005) A high-throughput inducible RNAi vector for plants. Plant Biotechnol J 3:583–590

Yamada H, Suzuki T, Terada K, Takei K, Ishikawa K, Miwa K, Yamashino T, Mizuno T (2001) The *Arabidopsis* AHK4 histidine kinase is a cytokinin-binding receptor that transduces cytokinin signals across the membrane. Plant Cell Physiol 42:1017–1023

Zubko E, Adams CJ, Macháčková I, Malbeck J, Scollan C, Meyer P (2002) Activation tagging identifies a gene from *Petunia hybrida* responsible for the production of active cytokinins in plants. Plant J 29:797–808